Photoluminescence at room temperature in disordered Ba 0.50 Sr 0.50 (Ti 0.80 Sn 0.20) O 3 thin films

I. A. Souza, A. Z. Simões, E. Longo, J. A. Varela, and P. S. Pizani

Citation: Applied Physics Letters **88**, 211911 (2006); doi: 10.1063/1.2206993
View online: http://dx.doi.org/10.1063/1.2206993
View Table of Contents: http://scitation.aip.org/content/aip/journal/apl/88/21?ver=pdfcov
Published by the AIP Publishing

Photoluminescence at room temperature in disordered $Ba_{0.50}Sr_{0.50}(Ti_{0.80}Sn_{0.20})O_3$ thin films

I. A. Souza,[a] A. Z. Simões, E. Longo, and J. A. Varela
Chemistry Institute, UNESP—Paulista State University, P.O. Box 355, 14801-970 Araraquara-SP, Brazil

P. S. Pizani
Department of Physics, UFSCar—São Carlos Federal University, P.O. Box 676, 13565-905 São Carlos-SP, Brazil

(Received 7 February 2006; accepted 13 April 2006; published online 25 May 2006)

Photoluminescence (PL) properties at room temperature of disordered $Ba_{0.50}Sr_{0.50}(Ti_{0.80}Sn_{0.20})O_3$ (BST:Sn) thin films were obtained by the polymeric precursor method. X-ray diffraction data and corresponding PL properties have been measured using the 488 nm line of an argon ion laser. The PL spectra of the film annealed at 350 °C for 21 h are stronger than those of the film annealed at 350 °C for 28 h, indicating a disorganized structure. The energy band gaps of the crystalline and amorphous BST:Sn thin films were 3.35 and 2.25 eV, respectively. The doped BST thin films also tend to a cubic structure, resulting from TiO_6 deformations. © *2006 American Institute of Physics*. [DOI: 10.1063/1.2206993]

The development of semiconductor materials with active optical properties such as photoluminescence (PL), electroluminescence, or nonlinear optic properties may lead to optoelectronic devices with superior performance. Much interest has been evinced in the study of PL in amorphous or nanostructured materials since visible PL at room temperature was observed in porous silicon.[1] In perovskite-type crystals, a broad luminescence band is usually observed at low temperatures and is associated to the presence of imperfections or defects.[2] These properties have led to renewed interest in the luminescence properties of semiconducting titanate compounds. For this reason, amorphous semiconductor compounds such as $BaTiO_3$ and $SrTiO_3$ appear particularly promising, since amorphous solids can present greater numbers of imperfections and can be produced at low temperature by chemical processes such as sol gel. Many reports have been published about investigations of the luminescence of perovskite-type compounds of both bulk and nanometer sizes in the form of crystalline structures,[3–5] but little or no information is available about the effects of amorphous thin films of the perovskite-type structure compounds. Meng *et al.*[6] observed in nanocrystalline $BaTiO_3$ a visible emission band at 514.5 nm line being its nature and origin attributed to the recombination of self-trapped excitons. Zhang *et al.*[7] investigated the PL in nanostructured Er^{+3}-doped $BaTiO_3$ crystalline films prepared by sol-gel method; a luminescence at 154 nm was achieved under excitation of both 514 and 980 nm lasers. Nanocrystalline barium titanate was synthesized by hydrothermal technique by Zhang *et al.*[8] and strong PL was observed centered at 696 nm, which was attributed to charge transfer via intrinsic defects inside oxygen octahedron. Pizani *et al.*[9] recently reported efficient room temperature PL in amorphous $BaTiO_3$ (a-$BaTiO_3$) powders. In that work, a simple chemical process was used to process the powders at a low temperature ($T<400$ °C). In addition, the PL peak position of this material was observed to depend on the exciting wavelength. Among the perovskite-type compounds, $Ba_xSr_{1-x}TiO_3$, $x=0-1$, in the powder and thin film forms, has been exhaustively investigated owing to its high dielectric constant coupled with its good thermal stability. However, its PL properties have not yet been reported. In this study, we present the results of PL measurements on $Ba_{0.50}Sr_{0.50}Ti_{0.80}Sn_{0.20}O_3$ (BST:Sn) thin films heat treated at various temperatures. Titanium isopropoxide (Hulls AG), strontium carbonate (Aldrich), barium carbonate (Aldrich), and tin chloride (Aldrich) were used as raw materials. The precursor solutions of barium, titanium, strontium, and tin were prepared by adding the raw materials to ethylene glycol and concentrate aqueous citric acid under heating and stirring. We reported studies of BST:Sn with the appropriate amount of Ti, Sr, Ba, and Sn solutions that were mixed and homogenized by stirring at 90 °C. The molar ratio of metal:citric acid:ethylene glycol was 1:4:16. The viscosity of the resulting solution was adjusted to 15 cP, controlling the water content using a Brookfield viscosimeter. From this solution the films were deposited by the spin-coating technique on (111) $Pt/Ti/SiO_2/Si$ substrates. A platinum layer (140 nm) was used as bottom electrode. The BST:Sn films were then annealed at 350 °C for 14, 21, and 28 h and at 700 °C for 2 h in oxygen atmosphere, resulting in all cases a film thickness of approximately 500 nm. Phase analysis of the films was performed at room temperature by x-ray powder diffraction (XRD) using a Bragg-Brentano diffractometer (Rigaku 2000) and Cu $K\alpha$ radiation. Microstructural characterization was performed by atomic force microscopy (AFM) to obtain a three-dimensional (3D) image reconstruction of the sample surface (Digital Instruments Multi-Mode Nanoscope-IIIa). The film thickness was measured by a thin film cross-section analysis made by scannig electron microscope (SEM) (Zeiss, DSM940A). The PL spectra of the BST:Sn thin films were taken with a U1000 Jobin-Yvon double monochromator coupled to a cooled GaAs photomultiplier and a conventional photon counting system. The 488.0 nm exciting wavelength of an argon ion laser was used, with the laser's maximum output power kept at 20 mW. A cylindrical lens was used to prevent the sample from overheating. The slit width used was 100 μm. All mea-

[a]Electronic mail: iedo-souza@uol.com.br

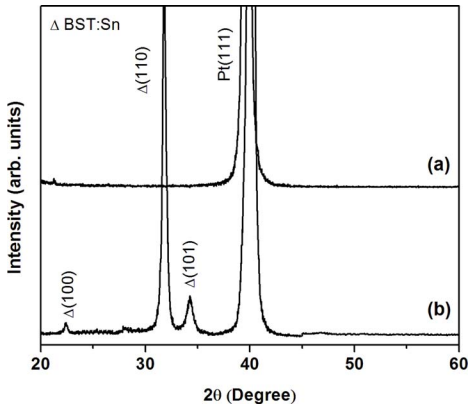

FIG. 1. (Color online) XRD patterns for disordered BST:Sn thin film (a) annealed at 350 °C for 28 h and (b) annealed at 700 °C for 2 h.

surements were taken at room temperature. The spectral dependence of the optical absorbance of the crystalline and amorphous BST:Sn thin films was taken at room temperature using a Cary 5G equipment.

Figure 1 shows the evolution of the XRD patterns of BST:Sn thin films prepared by the polymeric precursor method (PPM), deposited on platinum-coated silicon substrate, and annealed at 350 °C for 28 h and at 700 °C for 2 h in oxygen atmosphere. A diffuse XRD pattern can be observed at the temperature of 350 °C for 28 h, indicating the formation of an inorganic amorphous precursor after the pyrolysis process. After heat treatment at 700 °C for 2 h, the diffraction patterns of the films showed a well-crystallized structure. All the peaks are attributed to a pseudocubic perovskite structure except those ascribed to the Pt substrate. The BST:Sn thin films tend to a pseudocubic structure on average, but locally shows slight distortions resulted from TiO_6 which occurs at a short distance.

Figures 2(a) and 2(b) show three-dimensional images of a BST:Sn film annealed at 350 °C for 28 h and at 700 °C for 2 h in oxygen atmosphere, respectively. The amorphous thin film was characterized by a smooth surface with a homogeneous, crack-free microstructure, i.e., the surface was devoid of hillocks and the structure of granularity. The surface roughness was 0.75 nm. The surface morphology of the BST:Sn changes dramatically at high temperatures. At this stage of growth, coalescence of nuclei occurs, with formation of granular structures resulting in a significant increase in roughness. This result is in agreement with the XRD analysis, where at 700 °C for 2 h a high crystallization was observed.

Figure 3 shows the PL behavior observed in the amorphous and crystalline BST:Sn thin films with an exciting wavelength of 488.0 nm at room temperature. PL characteristics showed a broad intense luminescence in the visible region for amorphous materials, with maximum at about 550 nm. As illustrated in the PL spectra, when the annealing time was increased (under isothermal conditions), the intensity of PL increases. Increasing the heat treatment times causes a decrease in the total carbon material content. If the PL behavior observed comes from the disordered inorganic phases, more intense PL must occur for the material submitted to heat treatment in oxygen for a longer time. When the material is annealed at high temperatures, the PL intensity is virtually zero at room temperature and at liquid nitrogen temperature. This behavior can be explained as follows. As

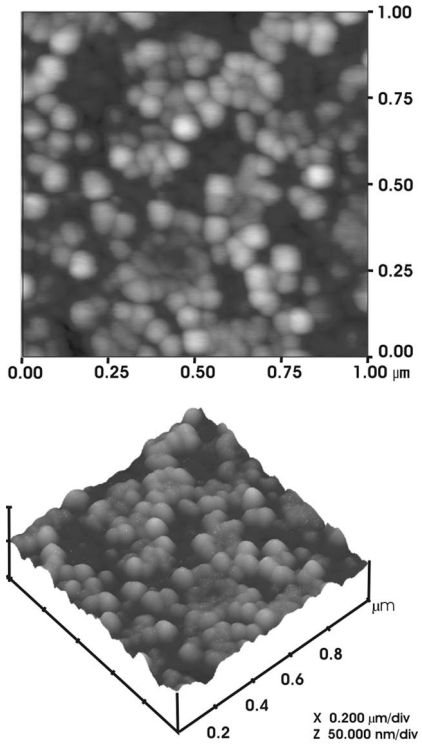

FIG. 2. AFM micrographies for BST:Sn thin film (a) annealed at 350 °C for 28 h and (b) annealed at 700 °C for 2 h.

the material begins to become ordered (in crystalline form), the intensity of photoluminescence drops to virtually zero at room temperature. Thus, if the photoluminescent signal is correlated with the disordered structure (BST:Sn amorphous thin film), it is generally believed that, when the system becomes ordered, the photoluminescent signal disappears, an assumption that is confirmed by the curve in Fig. 2. Therefore, there is a strong indication that the disordered phase (amorphous phase) is responsible for the PL phenomena.

Figures 4(a) and 4(b) illustrate the spectral dependence of absorbance for the BST:Sn film annealed at 350 °C for 28 h and at 700 °C for 2 h in oxygen atmosphere. The film annealed at 350 °C for 28 h showed a spectral dependence on absorbance similar to that found in amorphous semiconductors such as amorphous silicon (Si) and insulators, while crystalline film showed a typical interband transition of crys-

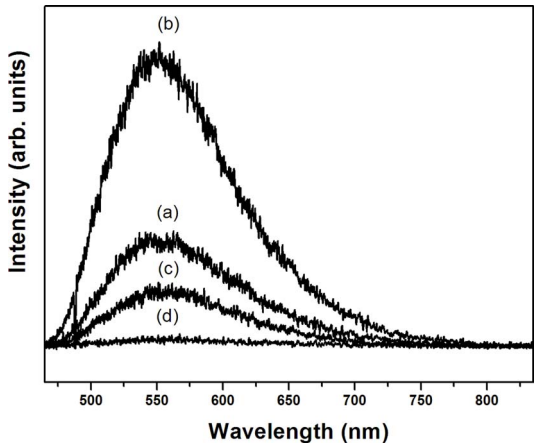

FIG. 3. (Color online) Room temperature photoluminescence spectra of BST: Sn thin films annealed at (a) 350 °C for 14 h, (b) 350 °C for 21 h, (c) 350 °C for 28 h, and (d) 700 °C for 2 h.

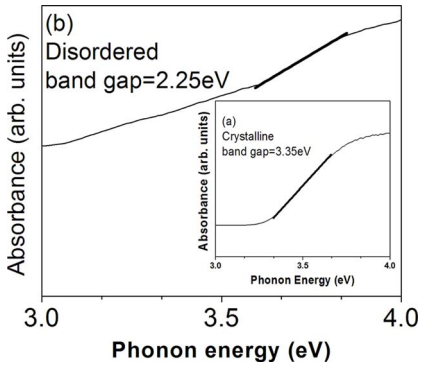

FIG. 4. (Color online) UV-vis absorbance spectra for (a) crystalline and (b) disordered BST:Sn thin films.

talline materials. In addition, in the high energy region of the absorbance curve (Fig. 3) the optical energy band gap is related to the absorbance and to the photon energy by the Tauc equation.[10] The energy band gaps of the crystalline and amorphous BST:Sn thin films were calculated to be 3.35 and 2.25 eV, respectively. These results show that our data are consistent with the interpretation that the exponential optical absorption edge and the optical band gap are controlled by the degree of disorder, structural and thermal, in the lattice of BST:Sn thin film. The polarity change caused by the Sn^{4+} addition in the BST plays a significant role in the PL. This decrease in the band gap can be ascribed to defects or impurities that give rise to intermediary levels of energy in the range of the band gap promoted by the BST:Sn disordered structure. As the band gap energies are much higher than the excitation energy that is used for collecting the PL spectra (2.54 eV), the mechanism giving rise PL is not a band to band process. These observations confirm the fact that PL is directly related to the localized states existing in the band gap. Montoncello *et al.*[11] pointed out that PL often highlights features that absorption measurements would rarely define, such as the properties of the energy levels lying within the band gap of a material. The model proposed by Blasse and Grabmaier[12] is based on a charge transfer from the atom having its main contribution in the valence band to the atom forming the conduction band. According to the hypothesis of Korzhik *et al.*[13] vacant localized states linked to local defects such as oxygen vacancies exist in the band gap above the valence band and below the conduction band.[14] In the model presented by Leonelli and Brebner,[15] some of the electrons promoted to the conduction band by absorption of photon form small polarons. The polaron interacts with holes trapped in the crystal (defect or impurities) and form self-trapped excitons (STE). In our model, the most important events occur before excitation. The structural and intermediate defects of the localized states in the band gap and inhomogeneous charge distribution polarization in the disordered system allow the trapping of electrons.[16] This model is not only consistent with the experimental data but also allows to explain the relation between structural disorder and PL at room temperature. As conclusion, low cost soft-chemical processing was used to prepare the BST:Sn thin films on $Pt/Ti/SiO_2/Si$ substrates, which displayed an intense broad photoluminescence at room temperature in the visible range in the structurally disordered material. The intense room temperature visible PL of noncrystalline BST:Sn thin films is discussed. The energy band gaps of the crystalline and amorphous BST:Sn thin films were 3.35 and 2.25 eV, respectively. The doped BST:Sn thin films also tend to a cubic structure, resulting from TiO_6 deformations. The structural and intermediate defects of the localized states in the band gap and inhomogeneous charge distribution in the cell allow the trapping of electrons. These findings may give rise to an alternative method to process nanostructured wide band gap semiconductors showing PL at room temperature.

The authors gratefully acknowledge the financial support of the Brazilian agencies FAPESP, CNPq, and CAPES. The authors thank the institutions CEFET-MA and UEMA.

[1] L. T. Canham, Appl. Phys. Lett. **57**, 1046 (1990).
[2] W. F. Zhang, Z. Yin, M. S. Zhang, Z. L. Du, and C. W. Chen, J. Phys.: Condens. Matter **11**, 5655 (1999).
[3] A. M. Van de Craats, G. J. Dirksen, and G. Blasse, J. Solid State Chem. **118**, 337 (1995).
[4] Z. Bryknar, V. Trepakov, Z. Potucek, and L. Jastrabik, J. Lumin. **87**, 605 (2000).
[5] J. Ballato, R. Esmacher, R. Schwartz, and M. Dejneka, J. Lumin. **86**, 101 (2000).
[6] J. Meng, Y. Huang, W. Zhang, Z. Du, Z. Zhu, and G. Zou, Phys. Lett. A **205**, 72 (1995).
[7] H. X. Zhang, C. H. Kam, Y. Zhou, X. Q. Han, Q. Xiang, S. Buddhudu, Y. L. Lam, and Y. C. Chan, J. Alloys Compd. **308**, 134 (2000).
[8] M. S. Zhang, Z. Yin, Q. Chen, W. Zhang, and W. Chen, Solid State Commun. **119**, 659 (2001).
[9] P. S. Pizani, E. R. Leite, F. M. Pontes, E. C. Paris, Z. J. H. Rangel, E. J. H. Lee, E. Longo, P. Delega, and J. A. Varela, Appl. Phys. Lett. **77**, 824 (2000).
[10] D. L. Wood and J. Tauc, Phys. Rev. B **5**, 3144 (1972).
[11] F. Montoncello, M. C. Carotta, B. Cavicchi, M. Ferroni, A. Giberti, V. Guidi, C. Malagu, G. Martinelli, and F. Meinardi, J. Appl. Phys. **94**, 1501 (2003).
[12] G. Blasse and B. C. Grabmaier, *Luminescent Materials* (Springer, Berlin, 1994).
[13] M. V. Korzhik, V. B. Pavlenko, T. N. Timoschenko, V. A. Katchanov, A. V. Singovskii, A. N. Annenkov, V. A. Liun, I. M. Solskii, and J. P. Peigneux, Phys. Status Solidi A **154**, 779 (1996).
[14] D. Kan, T. Terashima, R. Kanda, A. Maisuno, K. Tanaka, S. Chu, H. Kau, A. Ishizumi, Y. Kanemitsu, Y. Shimakawa, and M. Takano, Nat. Mater. **4**, 816 (2005).
[15] R. Leonelli and J. L. Brebner, Phys. Rev. B **33**, 8649 (1986).
[16] E. Longo, E. Orhan, F. M. Pontes, C. D. Pinheiro, E. R. Leite, J. A. Varela, P. S. Pizani, and A. Beltran, Phys. Rev. B **69**, 125115 (2004).